

1 **LxxIxE-like Motif in Spike Protein of SARS-CoV-2 that is Known to Recruit the Host**
2 **PP2A-B56 Phosphatase Mimics Artepillin C, an Immunomodulator, of Brazilian Green**
3 **Propolis**

4

5 Halim Maaroufi

6 Institut de biologie intégrative et des systèmes (IBIS). Université Laval. Québec, Canada.

7 Halim.maaroufi@ibis.ulaval.ca

8

9 **ABSTRACT**

10 SARS-CoV-2 is highly contagious and can cause acute respiratory distress syndrome (ARDS) and
11 multiple organ failure that are largely attributed to the cytokine storm. The surface coronavirus
12 spike (S) glycoprotein is considered as a key factor in host specificity because it mediates infection
13 by receptor-recognition and membrane fusion. Here, the analysis of SARS-CoV-2 S protein
14 revealed two B56-binding LxxIxE-like motifs in S1 and S2 subunits that could recruit the host
15 protein phosphatase 2A (PP2A). The motif in S1 subunit is absent in SARS-CoV and MERS-CoV.
16 Phosphatases and kinases are major players in the regulation of pro-inflammatory responses during
17 pathogenic infections. Moreover, studies have shown that viruses target PP2A in order to
18 manipulate host's antiviral responses. Recent researches have indicated that SARS-CoV-2 is
19 involved in sustained host inflammation. Therefore, by controlling acute inflammation, it is
20 possible to eliminate its dangerous effects on the host. Among efforts to fight COVID-19, the
21 interaction between LxxIxE-like motif and the PP2A-B56-binding pocket could be a target for the
22 discovery and/or development of a bioactive ligand inhibitor for therapeutic purposes. Indeed, a
23 small molecule called Artepillin C (ArtC), a main compound in Brazilian honeybee green propolis,
24 mimics the side chains of LxxLxE motif. Importantly, ArtC is known, among other effects, to have
25 anti-inflammatory activity that makes it an excellent candidate for future clinical trials in COVID-
26 19 patients.

27

28 **KEYWORDS** SARS-CoV-2; spike glycoprotein; PP2A-B56 phosphatase; LxxIxE-like motif;
29 anti-inflammation; Artepillin C.

30 INTRODUCTION

31
32 In March 11th 2020, the World Health Organization (WHO) announced that COVID-19
33 (Coronavirus Disease-2019) situation is a pandemic. The novel SARS-CoV-2 has had serious
34 consequences for human health and socioeconomic stability worldwide. Coronaviruses (CoVs) are
35 a large family of enveloped single positive-stranded RNA viruses that can infect both mammalian
36 and avian species because their rapid mutation and recombination facilitate their adaptation to new
37 hosts (Graham and Baric, 2010; Li, 2013). They can cause severe, often fatal Acute Respiratory
38 Distress Syndrome (ARDS). CoVs are classified into *Alpha*-, *Beta*-, *Gamma*-, and
39 *Deltacoronavirus* genetic genera. The novel betacoronavirus (betaCoVs) SARS-CoV-2 is
40 relatively close to other betaCoVs: severe acute respiratory syndrome coronavirus (SARS-CoV),
41 Middle East respiratory syndrome coronavirus (MERS-CoV), bat coronavirus HKU4, mouse
42 hepatitis coronavirus (MHV), bovine coronavirus (BCoV), and human OC43 coronavirus (HCoV-
43 OC43). SARS-CoV emerged in China (2002–2003) and spread to other countries (more than 8,000
44 infection cases and a fatality rate of ~10%) (Peiris et al., 2003). In 2012, MERS-CoV was detected
45 in the Middle East. It spread to multiple countries, infecting more than 1,700 people with a fatality
46 rate of ~36% (de Wit et al., 2016).

47
48 The surface-located SARS-CoV-2 spike glycoprotein S (S) is a 1273 amino acid residues. It is a
49 homotrimeric, multidomain, and integral membrane protein that give coronaviruses the appearance
50 of having crowns (*Corona* in Latin) (Li, 2016). It is a key piece of viral host recognition (receptor-
51 recognition) and organ tropism and induces strongly the host immune reaction (Li, 2015). It is
52 subdivided to S1 subunit that binds to a receptor on the host cell surface and S2 subunit that permits
53 viral and host membranes fusion. S1 subunit is divided into two domains, an N-terminal domain
54 (NTD) and a C-terminal receptor-binding domain (RBD) that can function as viral receptors-
55 binding (Li, 2012). In addition, S1 subunit is normally more variable in sequence among different
56 CoVs than is the S2 subunit (Masters, 2006).

57
58 Protein phosphatase 2A (PP2A) is a major family of Serine/Threonine phosphatases in eukaryotic
59 cells and regulates diverse biological processes through dephosphorylation of numerous signaling
60 molecules. PPA2 and phosphatase 1 (PP1), regulates over 90% of all Ser/Thr dephosphorylation

61 events in eukaryotic cells (Eichhorn et al., 2009). PP2A is a heterotrimeric holoenzyme composed
62 of a stable heterodimer of the scaffold A-subunit (PP2A-A) and catalytic C-subunit (PP2A-C) and
63 a variable mutually exclusive regulatory subunit from four families (B (B55), B' (B56), B'' and B''')
64 which provide substrate specificity. The human B56 family consists of at least five different
65 members (α , β , γ , δ and ϵ). Phosphatases and kinases are big players in the regulation of pro-
66 inflammatory responses during microbial infections. Sun et al. (2017) showed that PP2A plays an
67 important role in regulating inflammation by controlling the production of inflammatory
68 cytokines/chemokines (Kozicky and Sly, 2015). In addition, PP2A is one of the phosphatases
69 involved in negatively regulating the inflammatory response (Shanley et al., 2001). Moreover,
70 studies have revealed that viruses use multiple strategies to target PP2A in the aim to manipulate
71 host antiviral responses (Guergnon et al., 2011).

72
73 Artepillin C (ArtC) is uniquely found in Brazilian honeybee green propolis and is one of its major
74 bioactive components (Marcucci et al., 2001; Park et al., 2004). It is a low-molecular weight
75 phenolic single ring with two prenyl groups (3,5-diprenyl-4-hydroxycinnamic acid) (Szliszka et
76 al., 2013). These properties suggest high oral bioavailability and cell-permeability allowing good
77 biological activity of ArtC (Shimizu et al., 2004; Konishi et al. 2005; Konishi, 2005). Indeed,
78 Paulino et al. (2008) showed that ArtC exhibited bioavailability by oral administration in mice.
79 Interestingly, ArtC has many therapeutic effects, anti-microbial, anti-tumor, apoptosis-inductor,
80 immunomodulatory, and anti-oxidant effects (Salomão et al., 2004; Kimoto et al., 2001; Orsolich et
81 al., 2006; Matsuno et al., 1997; Gekker et al., 2005; Nakanishi et al., 2003). Many of these
82 therapeutic effects can be attributed to its immunomodulatory functions (Chan et al., 2013; Cheung
83 et al., 2011; Paulino, et al., 2008). Indeed, Szliszka et al., (2013) have tested the anti-inflammatory
84 activity of ArtC in activated RAW264.7 macrophages. They found that ArtC exerted strong
85 antioxidant activity and significantly inhibited the production of several pro-inflammatory
86 cytokines, such as TNF- α , IL-1 β and IL-12, which makes ArtC an excellent anti-inflammatory
87 drug. In addition, ArtC suppresses T cell proliferation and activation (Chan et al., 2013). Here, S
88 protein was analyzed because of its importance in mediating infection. This analysis revealed two
89 B56-binding LxxIx β E-like motifs in S1 and S2 subunits that could recruit the host PP2A.
90 Interestingly, side chains of LxxLxE motif present similarity with a small molecule called
91 Artepillin C (ArtC), a main compound in Brazilian honeybee green propolis. Moreover, ArtC has

92 anti-inflammatory activity that makes it an excellent candidate for future clinical trials in COVID-
93 19 patients.

94

95 **RESULTS AND DISCUSSION**

96

97 *Two LxxIxE-like motifs in S1 and S2 subunits of Spike protein*

98

99 Sequence analysis of SARS-CoV-2 spike protein by the eukaryotic linear motif (ELM) resource
100 (<http://elm.eu.org/>) revealed short linear motifs (SLiMs) known as LxxIxE-like motif
101 ,²⁹³LDPLSE²⁹⁸ in S1 subunit and ¹¹⁹⁷LIDLQE¹²⁰² in S2 subunit (Fig. 1). SLiMs are few amino
102 acid residues (3-15) in proteins that facilitate protein sequence modifications and protein-protein
103 interactions (Davey et al., 2012; Van Roey et al., 2014). RNA viruses are known to mutate quickly
104 and thus are able to create mimic motifs, on very short time scales, that could hijack biological
105 processes in the host cell such as cell signaling networks (Davey et al., 2015; Via et al., 2015;
106 Davey et al., 2011). Interestingly, ²⁹³LDPLSE²⁹⁸ is only present in SARS-CoV-2 and absent in S
107 protein of coronaviruses analysed in this study (Fig. 1A). In order to interact with protein(s),
108 ²⁹³LDPLSE²⁹⁸ must be present at the surface of S1 subunit. Indeed, this motif is exposed in the
109 surface of S1 subunit in the end of NTD (Fig. 3B). A second motif ¹¹⁹⁷LIDLQE¹²⁰² is present in S2
110 subunit and conserved in SARS-CoV-2, SARS-CoV, SARS-like of bat from China and Kenya (Fig.
111 1B). These last betacoronaviruses are phylogenetically close (Fig. 2). Unfortunately, the region
112 containing ¹¹⁹⁷LIDLQE¹²⁰² peptide has not been resolved in all known 3D structures of S protein
113 to know if it is exposed in the surface. Probably, ¹¹⁹⁷LIDLQE¹²⁰² peptide is in an intrinsic
114 disordered region of S protein.

115

116 *Artepillin C, anti-inflammatory compound, mimics LxxLxE motif in S protein*

117

118 In order to find small molecules with substituents that topologically and structurally resemble key
119 amino acid side chains in LxxLxE motif, the method developed by Baran et al. (2007) has been
120 used. This method allowed to discover a small molecule called Artepillin (ArtC) (Fig. 4A). It is a
121 low-molecular weight phenolic single ring with two prenyl groups (3,5-diprenyl-4-
122 hydroxycinnamic acid) (Szliszka et al., 2013). Figure 4B shows that the side chains of the two
123 leucine and glutamic acid that constitute the key amino acid side chains are superimposed with the
124 two prenyl groups and acid group of ArtC, respectively. ArtC is uniquely found in Brazilian

125 honeybee green propolis and is one of its major bioactive components (Marcucci et al., 2001; Park
126 et al., 2004). In addition, it has many therapeutic effects, anti-microbial, anti-tumor, apoptosis-
127 inductor, immunomodulatory, and anti-oxidant effects (Salomão et al., 2004; Kimoto et al., 2001;
128 Orsolic et al., 2006; Matsuno et al., 1997; Gekker et al., 2005; Nakanishi et al., 2003). Many of
129 these therapeutic effects can be attributed to its immunomodulatory functions (Chan et al., 2013;
130 Cheung et al., 2011; Paulino, et al., 2008).

131
132 *Interactions of ²⁹³LDPLSE²⁹⁸ and ArtC with B56 regulatory subunit*

133
134 In order to determine the molecular interactions of ²⁹³LDPLSE²⁹⁸ and ArtC with B56 regulatory
135 subunit of PP2A (PP2A-B56), molecular docking was performed with the software AutoDock vina
136 (Trott and Olson, 2010). Figure 4C and D show that ²⁹³LDPLSE²⁹⁸ peptide is localized in the same
137 region as pS-RepoMan peptide that contains the LxxIx \bar{E} motif (PDBid: 5SW9_B) and important
138 amino acids of LxxIx \bar{E} -like motif are superimposed with those of pS-RepoMan peptide (Fig. 4D).
139 That is confirmed the reliability of AutoDock vina peptide docking module. In addition, Leu293
140 of ²⁹³LDPLSE²⁹⁸ is docked into hydrophobic pocket and Glu298 form ionic interactions with amino
141 acid residues in positive charged region of PP2A-B56 (Fig. 4C). Note that ²⁹³LDPLSE²⁹⁸ contains
142 a serine that could be phosphorylated generating a negative charge that will interact with positive
143 patch in B56 subunit, enhancing binding affinity (Nygren and Scott, 2015). In the case of ArtC, its
144 two prenyl groups are docked into two pockets as already seen with ²⁹³LDPLSE²⁹⁸ peptide (Fig.
145 4E-F). Note that the side chain of carboxylic acid group of ArtC is short to form ionic interactions
146 with amino acid residues in positive charged region of PP2A-B56 (Fig. 4E). Therefore, to enhance
147 binding affinity of ArtC, it is necessary to increase the length of side chain of carboxylic acid group.
148 Interestingly, by using PinaColada, a computational method (Zaidman and Wolfson, 2016) for the
149 design and affinity improvement of peptides that preclude protein-protein interaction, the peptide
150 predicted (²⁹³LIDLEE²⁹⁸) by the software is mutated in C-terminal to negative charge residue
151 (glutamic acid), showing the importance of the negative charge of peptide to interact with PP2A-
152 B56. According to Autodock software, predicted binding affinity of ²⁹³LDPLSE²⁹⁸ is -4.9 Kcal/mol,
153 and this of ArtC is -6.1 Kcal/mol. It is known that the binding affinity of SLiMs is relatively weak
154 (low μ molar range) (Gouw et al., 2018). This suggests that ArtC could compete with the virus to
155 bind to PP2A-B56. To my knowledge, no compound has been identified to interact with regulatory
156 subunits of PP2A, in addition it is the first time that a small molecule has been found that mimics

157 the LxxIxE motif. Despite of numerous studies on ArtC its target is not yet known. In this study,
158 its target is predicted as B56-PP2A. In general, activation of PP2A appears to have a suppressive
159 effect on the inflammatory response (Sun et al., 2017). This suggests according to anti-
160 inflammatory effect of ArtC that it could activate, *in vivo*, B56-PP2A.

161
162 *Protein phosphatase 2A and single RNA viruses*
163
164 It has been shown in single RNA viruses, Ebola virus (EBOV) and Dengue fever virus (DENV)
165 that they recruit the host PP2A through its regulatory subunit B56-binding LxxIxE motif to activate
166 transcription and replication (Kruse et al., 2018; Oliveira et al., 2018). In addition, it has been
167 shown an exacerbation of lung inflammation in mice infected with rhinovirus 1B (the most
168 common viral infectious agent in humans). Administrating Salmeterol (beta-agonist) treatment to
169 mice exerts anti-inflammatory effects by interacting with catalytic subunit PP2A, thus increasing
170 its activity. It is probable that beta-agonists have the potential to target distinct pro-inflammatory
171 pathways unresponsive to corticosteroids in patients with rhinovirus-induced exacerbations
172 (Hatchwell et al., 2014). Treatment with Salmeterol drug may merit investigation for the possibility
173 of using it in COVID-19's patients with sustained and dangerous inflammatory reaction.

174
175 *Summary and conclusion*
176
177 Analysis of SARS-CoV-2 proteome in the search of SLiMs that could be used by SARS-CoV-2 to
178 manipulate host, allowed to discover in S protein an LxxIxE-like motif that is known to recruit the
179 host PP2A-B56 phosphatase. Interestingly, PP2A is involved in the regulation of pro-inflammatory
180 responses during pathogen infections. Well, recent researches have indicated that SARS-CoV-2 is
181 involved in sustained host inflammation. Therefore, by controlling acute inflammation, it is
182 possible to eliminate its dangerous effects on the host. LxxIxE motif of CoV-2 allowed to find a
183 small molecule called Artepillin (ArtC), a main compound in Brazilian honeybee green propolis,
184 which is known to have anti-inflammatory activity. ArtC, by its non-cytotoxicity in cells, high oral
185 bioavailability, tested in mice, and cell-permeability, in addition that it can be synthesized in the
186 laboratory (Uto et al., 2002; Yashiro et al., 2015) and produced in yeast by using synthetic biology
187 (Munakata et al., 2019) makes it an ideal molecule for future clinical trials in COVID-19 patients.

188

189 **MATERIALS AND METHODS**

190

191 *Sequence analysis*

192

193 To search probable short linear motifs (SLiMs), SARS-CoV-2 spike protein sequence was scanned
194 with the eukaryotic linear motif (ELM) resource (<http://elm.eu.org/>).

195 In the aim to find small molecules containing amino acids substituents that mimic LxxIxE-like
196 motif, method described by Baran et al. (2007) was used.

197

198 *3D modeling and molecular docking*

199

200 3D structure of Artepillin C (ArtC) was obtained from PubChem database:
201 <https://pubchem.ncbi.nlm.nih.gov/compound/5472440#section=3D-Conformer>.

202 For docking, the coordinates of the ²⁹³LDPLSE²⁹⁸ peptide were extracted from spike S protein of
203 CoV-2 structure (PDBid: 6VSB_A). Unfortunately, the region containing ¹¹⁹⁷LIDLQE¹²⁰² peptide
204 has not been resolved in all known 3D structures of spike S protein. So, Pep-Fold (Thevenet et al.,
205 2012) software was used to model *de novo* this peptide. The model quality of the peptide was
206 assessed by analysis of a Ramachandran plot through PROCHECK (Vaguine et al., 1999).

207 The docking of the two peptides into B56 regulatory subunit of PPA2 (PDBid: 5SWF_A) was
208 performed with the software AutoDock vina (Trott and Olson, 2010). The 3D complex containing
209 B56 subunit and peptides was refined by using FlexPepDock (London et al., 2011), which allows
210 full flexibility to the peptide and side-chain flexibility to the receptor. The electrostatic potential
211 surface of the B56 subunit was realized with PyMOL software (<http://pymol.org/>).

212 PinaColada a computational method (Zaidman and Wolfson, 2016) for inhibitory peptide design
213 was used to improve affinity of ²⁹³LDPLSE²⁹⁸ peptide to bind to B56 regulatory subunit of PPA2.
214 The software mutates several times the input peptide in the aim to find the highest binding affinity.

215

216 *Phylogeny*

217

218 To establish the phylogenetic relationships between spike S protein of SARS-CoV-2 and
219 representative betacoronaviruses, amino acid residues sequences were aligned with Clustal omega
220 (Sievers et al., 2011) and a phylogenetic tree was constructed with MrBayes (Huelsenbeck and
221 Ronquist, 2001) using: Likelihood model (Number of substitution types: 6(GTR); Substitution

222 model: Poisson; Rates variation across sites: Invariable + gamma); Markov Chain Monte Carlo
223 parameters (Number of generations: 100 000; Sample a tree every: 1000 generations) and Discard
224 first 500 trees sampled (burnin).

225

226 **ACKNOWLEDGMENTS**

227 I would like to thank the IBIS bioinformatics group for their help. I am grateful to Dr. Ahmad
228 Abdel-Mawgoud SALEH, Université Laval, for the revision of the manuscript.

229

230 **CONFLICT OF INTERESTED**

231 The author declares that he has no conflicts of interest.

232

233 **REFERENCES**

234

235 Baran, I., Varekova, R. S., Parthasarathi, L., Suchomel, S., Casey, F., & Shields, D. C. (2007).
236 Identification of potential small molecule peptidomimetics similar to motifs in proteins. *J Chem*
237 *Inf Model*, 47(2), 464-474. doi:10.1021/ci600404q

238 Chan, G. C., Cheung, K. W., & Sze, D. M. (2013). The immunomodulatory and anticancer
239 properties of propolis. *Clin Rev Allergy Immunol*, 44(3), 262-273. doi:10.1007/s12016-012-8322-
240 2

241 Cheung, K. W., Sze, D. M., Chan, W. K., Deng, R. X., Tu, W., & Chan, G. C. (2011). Brazilian
242 green propolis and its constituent, Artepillin C inhibits allogeneic activated human CD4 T cells
243 expansion and activation. *J Ethnopharmacol*, 138(2), 463-471. doi:10.1016/j.jep.2011.09.031

244 Davey, N. E., Cyert, M. S., & Moses, A. M. (2015). Short linear motifs - ex nihilo evolution of
245 protein regulation. *Cell Commun. Signal.*, 13, 43. doi:10.1186/s12964-015-0120-z

246 Davey, N. E., Travé, G., & Gibson, T. J. (2011). How viruses hijack cell regulation. *Trends*
247 *Biochem. Sci.*, 36(3), 159-169. doi:10.1016/j.tibs.2010.10.002

248 Davey, N. E., Van Roey, K., Weatheritt, R. J., Toedt, G., Uyar, B., Altenberg, B., . . . Gibson, T.
249 J. (2012). Attributes of short linear motifs. *Mol. Biosyst.*, 8(1), 268-281. doi:10.1039/c1mb05231d

250 de Wit, E., van Doremalen, N., Falzarano, D., & Munster, V. J. (2016). SARS and MERS: recent
251 insights into emerging coronaviruses. *Nat. Rev. Microbiol.*, 14(8), 523-534.
252 doi:10.1038/nrmicro.2016.81

253 Eichhorn, P. J. A., Creighton, M. P., & Bernards, R. (2009). Protein phosphatase 2A regulatory
254 subunits and cancer. *Biochim. Biophys. Acta*, 1795(1), 1-15. doi:10.1016/j.bbcan.2008.05.005

- 255 Gekker, G., Hu, S., Spivak, M., Lokensgard, J. R., & Peterson, P. K. (2005). Anti-HIV-1 activity
256 of propolis in CD4(+) lymphocyte and microglial cell cultures. *J Ethnopharmacol*, *102*(2), 158-
257 163. doi:10.1016/j.jep.2005.05.045
- 258 Gouw, M., Michael, S., Sámano-Sánchez, H., Kumar, M., Zeke, A., Lang, B., . . . Gibson, T. J.
259 (2018). The eukaryotic linear motif resource - 2018 update. *Nucleic Acids Res.*, *46*(D1), D428-
260 D434. doi:10.1093/nar/gkx1077
- 261 Graham, R. L., & Baric, R. S. (2010). Recombination, reservoirs, and the modular spike:
262 mechanisms of coronavirus cross-species transmission. *J. Virol.*, *84*(7), 3134-3146.
263 doi:10.1128/JVI.01394-09
- 264 Guernon, J., Godet, A. N., Galioot, A., Falanga, P. B., Colle, J.-H., Cayla, X., & Garcia, A. (2011).
265 PP2A targeting by viral proteins: a widespread biological strategy from DNA/RNA tumor viruses
266 to HIV-1. *Biochim. Biophys. Acta*, *1812*(11), 1498-1507. doi:10.1016/j.bbadis.2011.07.001
- 267 Hatchwell, L., Girkin, J., Dun, M. D., Morten, M., Verrills, N., Toop, H. D., . . . Mattes, J. (2014).
268 Salmeterol attenuates chemotactic responses in rhinovirus-induced exacerbation of allergic airways
269 disease by modulating protein phosphatase 2A. *J. Allergy Clin. Immunol.*, *133*(6), 1720-1727.
270 doi:10.1016/j.jaci.2013.11.014
- 271 Huelsenbeck, J. P., & Ronquist, F. (2001). MRBAYES: Bayesian inference of phylogenetic
272 trees. *Bioinformatics*, *17*(8), 754-755. doi:10.1093/bioinformatics/17.8.754
- 273 Kimoto, T., Aga, M., Hino, K., Koya-Miyata, S., Yamamoto, Y., Micallef, M. J., . . . Kurimoto,
274 M. (2001). Apoptosis of human leukemia cells induced by Artepillin C, an active ingredient of
275 Brazilian propolis. *Anticancer Res*, *21*(1A), 221-228.
- 276 Konishi, Y. (2005). Transepithelial transport of artepillin C in intestinal Caco-2 cell
277 monolayers. *Biochim Biophys Acta*, *1713*(2), 138-144. doi:10.1016/j.bbamem.2005.05.011
- 278 Konishi, Y., Hitomi, Y., Yoshida, M., & Yoshioka, E. (2005a). Absorption and bioavailability of
279 artepillin C in rats after oral administration. *J Agric Food Chem*, *53*(26), 9928-9933.
280 doi:10.1021/jf051962y
- 281 Kozicky, L. K., & Sly, L. M. (2015). Phosphatase regulation of macrophage activation. *Semin*
282 *Immunol*, *27*(4), 276-285. doi:10.1016/j.smim.2015.07.001
- 283 Kruse, T., Biedenkopf, N., Hertz, E. P. T., Dietzel, E., Stalman, G., López-Méndez, B., . . . Becker,
284 S. (2018). The Ebola Virus Nucleoprotein Recruits the Host PP2A-B56 Phosphatase to Activate
285 Transcriptional Support Activity of VP30. *Mol. Cell*, *69*(1), 136-145.e136.
286 doi:10.1016/j.molcel.2017.11.034
- 287 Li, F. (2012). Evidence for a common evolutionary origin of coronavirus spike protein receptor-
288 binding subunits. *J. Virol.*, *86*(5), 2856-2858. doi:10.1128/JVI.06882-11
- 289 Li, F. (2013). Receptor recognition and cross-species infections of SARS coronavirus. *Antiviral*
290 *Res.*, *100*(1), 246-254. doi:10.1016/j.antiviral.2013.08.014

- 291 Li, F. (2015). Receptor recognition mechanisms of coronaviruses: a decade of structural studies. *J.*
292 *Virol.*, 89(4), 1954-1964. doi:10.1128/JVI.02615-14
- 293 Li, F. (2016). Structure, Function, and Evolution of Coronavirus Spike Proteins. *Annu Rev Virol*,
294 3(1), 237-261. doi:10.1146/annurev-virology-110615-042301
- 295 London, N., Raveh, B., Cohen, E., Fathi, G., & Schueler-Furman, O. (2011). Rosetta FlexPepDock
296 web server--high resolution modeling of peptide-protein interactions. *Nucleic Acids Res.*, 39(Web
297 Server issue), W249-253. doi:10.1093/nar/gkr431
- 298 Marcucci, M. C., Ferreres, F., García-Viguera, C., Bankova, V. S., De Castro, S. L., Dantas, A. P.,
299 . . . Paulino, N. (2001). Phenolic compounds from Brazilian propolis with pharmacological
300 activities. *J Ethnopharmacol*, 74(2), 105-112. doi:10.1016/s0378-8741(00)00326-3
- 301 Masters, P. S. (2006). The molecular biology of coronaviruses. *Adv. Virus Res.*, 66, 193-292.
302 doi:10.1016/S0065-3527(06)66005-3
- 303 Matsuno, T., Jung, S. K., Matsumoto, Y., Saito, M., & Morikawa, J. (1997). Preferential
304 cytotoxicity to tumor cells of 3,5-diprenyl-4-hydroxycinnamic acid (artepillin C) isolated from
305 propolis. *Anticancer Res*, 17(5A), 3565-3568.
- 306 Munakata, R., Takemura, T., Tatsumi, K., Moriyoshi, E., Yanagihara, K., Sugiyama, A., . . .
307 Yazaki, K. (2019). Isolation of. *Commun Biol*, 2, 384. doi:10.1038/s42003-019-0630-0
- 308 Nakanishi, I., Uto, Y., Ohkubo, K., Miyazaki, K., Yakumar, H., Urano, S., . . . Ikota, N. (2003).
309 Efficient radical scavenging ability of artemillin C, a major component of Brazilian propolis, and
310 the mechanism. *Org Biomol Chem*, 1(9), 1452-1454. doi:10.1039/b302098c
- 311 Nygren, P. J., & Scott, J. D. (2015). Therapeutic strategies for anchored kinases and phosphatases:
312 exploiting short linear motifs and intrinsic disorder. *Front. Pharmacol.*, 6, 158.
313 doi:10.3389/fphar.2015.00158
- 314 Oliveira, M., Lert-Itthiporn, W., Cavadas, B., Fernandes, V., Chuansumrit, A., Anunciação, O., . .
315 . Sakuntabhai, A. (2018). Joint ancestry and association test indicate two distinct pathogenic
316 pathways involved in classical dengue fever and dengue shock syndrome. *PLoS Negl. Trop. Dis.*,
317 12(2), e0006202. doi:10.1371/journal.pntd.0006202
- 318 Orsolić, N., Saranović, A. B., & Basić, I. (2006). Direct and indirect mechanism(s) of antitumour
319 activity of propolis and its polyphenolic compounds. *Planta Med*, 72(1), 20-27. doi:10.1055/s-
320 2005-873167
- 321 Park, Y. K., Paredes-Guzman, J. F., Aguiar, C. L., Alencar, S. M., & Fujiwara, F. Y. (2004).
322 Chemical constituents in *Baccharis dracunculifolia* as the main botanical origin of southeastern
323 Brazilian propolis. *J Agric Food Chem*, 52(5), 1100-1103. doi:10.1021/jf021060m
- 324 Paulino, N., Abreu, S. R., Uto, Y., Koyama, D., Nagasawa, H., Hori, H., . . . Bretz, W. A. (2008).
325 Anti-inflammatory effects of a bioavailable compound, Artemillin C, in Brazilian propolis. *Eur J*
326 *Pharmacol*, 587(1-3), 296-301. doi:10.1016/j.ejphar.2008.02.067

- 327 Peiris, J. S. M., Lai, S. T., Poon, L. L. M., Guan, Y., Yam, L. Y. C., Lim, W., . . . group, S. s.
328 (2003). Coronavirus as a possible cause of severe acute respiratory syndrome. *Lancet*, *361*(9366),
329 1319-1325. doi:10.1016/s0140-6736(03)13077-2
- 330 Salomão, K., Dantas, A. P., Borba, C. M., Campos, L. C., Machado, D. G., Aquino Neto, F. R., &
331 de Castro, S. L. (2004). Chemical composition and microbicidal activity of extracts from Brazilian
332 and Bulgarian propolis. *Lett Appl Microbiol*, *38*(2), 87-92. doi:10.1111/j.1472-765x.2003.01458.x
- 333 Shanley, T. P., Vasi, N., Denenberg, A., & Wong, H. R. (2001a). The serine/threonine phosphatase,
334 PP2A: endogenous regulator of inflammatory cell signaling. *J Immunol*, *166*(2), 966-972.
335 doi:10.4049/jimmunol.166.2.966
- 336 Shimizu, K., Ashida, H., Matsuura, Y., & Kanazawa, K. (2004). Antioxidative bioavailability of
337 artemillin C in Brazilian propolis. *Arch Biochem Biophys*, *424*(2), 181-188.
338 doi:10.1016/j.abb.2004.02.021
- 339 Sievers, F., Wilm, A., Dineen, D., Gibson, T. J., Karplus, K., Li, W., . . . Higgins, D. G. (2011).
340 Fast, scalable generation of high-quality protein multiple sequence alignments using Clustal
341 Omega. *Mol. Syst. Biol.*, *7*, 539. doi:10.1038/msb.2011.75
- 342 Sun, L., Pham, T. T., Cornell, T. T., McDonough, K. L., McHugh, W. M., Blatt, N. B., . . . Shanley,
343 T. P. (2017a). Myeloid-Specific Gene Deletion of Protein Phosphatase 2A Magnifies MyD88- and
344 TRIF-Dependent Inflammation following Endotoxin Challenge. *J Immunol*, *198*(1), 404-416.
345 doi:10.4049/jimmunol.1600221
- 346 Szliszka, E., Mertas, A., Czuba, Z. P., & Król, W. (2013). Inhibition of Inflammatory Response by
347 Artemillin C in Activated RAW264.7 Macrophages. *Evid Based Complement Alternat Med*, *2013*,
348 735176. doi:10.1155/2013/735176
- 349 Thévenet, P., Shen, Y., Maupetit, J., Guyon, F., Derreumaux, P., & Tufféry, P. (2012). PEP-FOLD:
350 an updated de novo structure prediction server for both linear and disulfide bonded cyclic
351 peptides. *Nucleic Acids Res.*, *40*(Web Server issue), W288-293. doi:10.1093/nar/gks419
- 352 Trott, O., & Olson, A. J. (2010). AutoDock Vina: improving the speed and accuracy of docking
353 with a new scoring function, efficient optimization, and multithreading. *J. Comput. Chem.*, *31*(2),
354 455-461. doi:10.1002/jcc.21334
- 355 Uto, Y., Hirata, A., Fujita, T., Takubo, S., Nagasawa, H., & Hori, H. (2002). First total synthesis
356 of artemillin C established by o,o'-diprenylation of p-halophenols in water. *J Org Chem*, *67*(7),
357 2355-2357. doi:10.1021/jo0056904
- 358 Vaguine, A. A., Richelle, J., & Wodak, S. J. (1999). SFCHECK: a unified set of procedures for
359 evaluating the quality of macromolecular structure-factor data and their agreement with the atomic
360 model. *Acta Crystallogr. D Biol. Crystallogr.*, *55*(Pt 1), 191-205.
361 doi:10.1107/S09074444998006684

362 Van Roey, K., Uyar, B., Weatheritt, R. J., Dinkel, H., Seiler, M., Budd, A., . . . Davey, N. E. (2014).
363 Short linear motifs: ubiquitous and functionally diverse protein interaction modules directing cell
364 regulation. *Chem. Rev.*, *114*(13), 6733-6778. doi:10.1021/cr400585q

365 Via, A., Uyar, B., Brun, C., & Zanzoni, A. (2015). How pathogens use linear motifs to perturb host
366 cell networks. *Trends Biochem. Sci.*, *40*(1), 36-48. doi:10.1016/j.tibs.2014.11.001

367 Yashiro, K., Hanaya, K., Shoji, M., & Sugai, T. (2015). New synthesis of artepillin C, a prenylated
368 phenol, utilizing lipase-catalyzed regioselective deacetylation as the key step. *Biosci Biotechnol*
369 *Biochem*, *79*(12), 1926-1930. doi:10.1080/09168451.2015.1058704

370 Zaidman, D., & Wolfson, H. J. (2016). PinaColada: peptide-inhibitor ant colony ad-hoc design
371 algorithm. *Bioinformatics*, *32*(15), 2289-2296. doi:10.1093/bioinformatics/btw133

372

373

374 **FIGURES LEGEND**

375

376 **Figure 1.** Multiple alignment of the spike glycoprotein of betacoronaviruses using Clustal omega.
377 ²⁹³LDPLSE²⁹⁸ (A) and ¹¹⁹⁷LIDLQE¹²⁰ (B) motifs are indicated by green stars. GenBank and
378 UniProt accession numbers are indicated at the start of each sequence. The figure was prepared
379 with ESPript (<http://esprict.ibcp.fr>).

380

381 **Figure 2.** Unrooted phylogenetic tree of spike protein of representative betacoronaviruses. The tree
382 was constructed using Mr Bayes method based on the multiple sequence alignment by Clustal
383 omega. Red rectangle assembles betacoronaviruses with the same ¹¹⁹⁷LIDLQE¹²⁰². Green star
384 indicated the only betacoronavirus with ²⁹³LDPLSE²⁹⁸. GenBank and UniProt accession numbers
385 are indicated at the start of each sequence.

386

387 **Figure 3.** Spike (S) protein of SARS-CoV-2. (A) Diagram representation of S protein colored by
388 domain. N-terminal domain (NTD), receptor-binding domain (RBD), subdomains 1 and 2 (SD1-
389 2, orange), S1/S2 protease cleavage site, Fusion peptide (FP), heptad repeat 1 and 2 (HR1 and
390 HR2), central helix (CH), connector domain (CD), transmembrane domain (TM), cytoplasmic tail
391 (CT), and the localization of ²⁹³LDPLSE²⁹⁸ in the end of NTD and ¹¹⁹⁷LIDLQE¹²⁰² peptide in
392 HR2. (B) Surface structure representation of the S1 subunit (PDBid: 6VSB_A). ²⁹³LDPLSE²⁹⁸
393 peptide is localized in the surface S1 subunit (red).

394
395 **Figure 4.** Stick representation of **(A)** Artepillin C (ArtC) and **(B)** superposition of ArtC (yellow)
396 and ²⁹³LDPLSE²⁹⁸ peptide (green). Electrostatic potential surface representation of the region of
397 the B56 regulatory subunit of PP2A (PDBid: 5SWF_A) with docked **(C)** ²⁹³LDPLSE²⁹⁸ peptide
398 (green), **(D)** ²⁹³LDPLSE²⁹⁸ superimposed to pS-RepoMan (orange)
399 (⁵⁸¹RDIASKKPLL**p**SPIPELPEVPE⁶⁰¹) peptide (PDBid: 5SW9_B), **(E)** ArtC (yellow) and **(F)** ArtC
400 superimposed to ²⁹³LDPLSE²⁹⁸ peptide (green). The surfaces are colored by electrostatic potential
401 with negative charge shown in red and positive charge in blue. Images were generated using PyMol
402 (www.pymol.org).
403

404

A

	270	280	290	300	310	320
YP_009724390.1_Human_SARS-CoV-2_Wuhan-Hu-1_China	VGYIQPR	TFLLKY	NENCT	ITDAVDC	ALDPL	SETKCT
P59594.1_Human_SARS-Cov_HongKong_China	VGYLKPT	TFMLKY	DENCT	ITDAVDC	SQNP	LAEKCS
ATO98205.1_Bat_SARS-like_coronavirus_China	VGYLKPA	TFMLKY	DENCT	ITDAVDC	SQNP	LAEKCS
APO40579.1_Bat_SARS-like_coronavirus_Kenya	VGHLLKPL	TMLAEF	DENCT	ITDAVDC	SQDP	LSEIKCT
P36334_Human_SPIKE_CVHOC_coronavirus_OC43	VTFLLTSR	QYLLAF	NQDCI	IFNAED	CMSDF	MSEIKCK
P25190_Bovine_SPIKE_CVBF_coronavirus_strain_F15	VTFLLTSR	QYLLAF	NQDCI	IFNAED	CMSDF	MSEIKCK
P11225_Murine_SPIKE_CVMJH_coronavirus_JHM	VTFLLTSR	QYLLAF	NQDCI	IFNAED	CMSDF	MSEIKCK
ALK80251.1_Human_MERS-CoV_South-Korea	VYKLLQPL	TFLLDF	SVDGY	IRRAID	CGFND	LSQLHCS
A3EX94_Bat_SPIKE_BCHK4_coronavirus_HKU4	VYKLLHQL	TYLLDF	SVDGY	IRRAID	CGHDD	LSQLHCS
QGA70702.1_Erinaceus_coronavirus_HKU31_China	TYQLHKL	NYLVEF	DVGCY	IVRASD	CGANDY	TQLCS

405

406

B

	1190	1200	1210	1220	1230	1240
YP_009724390.1_Human_SARS-CoV-2_Wuhan-Hu-1_China	NEVAKN	LNESL	IDLQ	ELGK	YEQY	IKWPWY
P59594.1_Human_SARS-Cov_HongKong_China	NEVAKN	LNESL	IDLQ	ELGK	YEQY	IKWPWY
ATO98205.1_Bat_SARS-like_coronavirus_China	NEVAKN	LNESL	IDLQ	ELGK	YEQY	IKWPWY
APO40579.1_Bat_SARS-like_coronavirus_Kenya	NEIAKN	LNESL	IDLQ	ELGK	YEQY	IKWPWY
P36334_Human_SPIKE_CVHOC_coronavirus_OC43	QEAIKV	LNQSY	INLKD	IGTYE	YV	KWPWY
P25190_Bovine_SPIKE_CVBF_coronavirus_strain_F15	QEAIKV	LNQSY	INLKD	IGTYE	YV	KWPWY
P11225_Murine_SPIKE_CVMJH_coronavirus_JHM	QDAIKK	LNQSY	INLKE	VGTYE	MY	VKWPWY
ALK80251.1_Human_MERS-CoV_South-Korea	QQVVK	LNDSY	IDLKE	LGNYT	YV	NKWPWY
A3EX94_Bat_SPIKE_BCHK4_coronavirus_HKU4	QEVVK	LNDSY	IDLKE	LGNYT	YV	NKWPWY
QGA70702.1_Erinaceus_coronavirus_HKU31_China	QSVVEA	LNQSY	IELK	ELGNYT	YV	NKWPWY

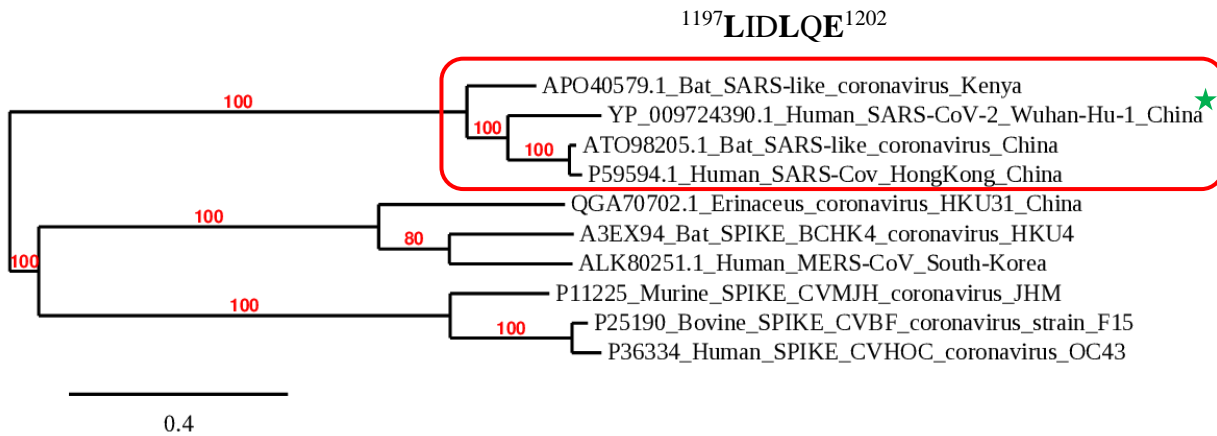
407

408 **Fig. 1**

409

410

411

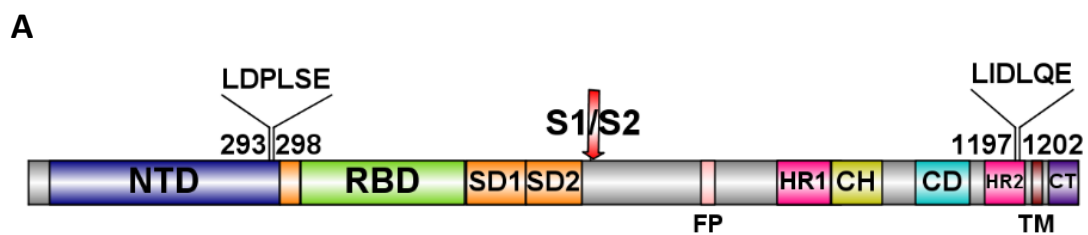


412

413 **Fig. 2**

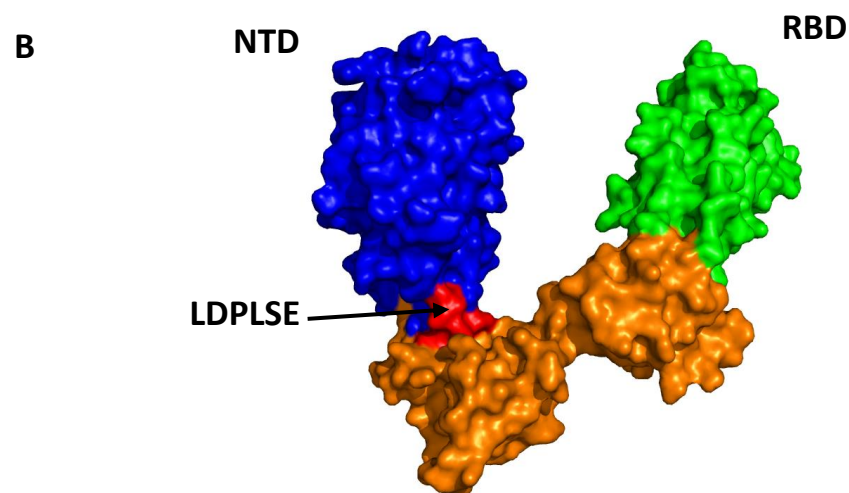
414

415



416

417

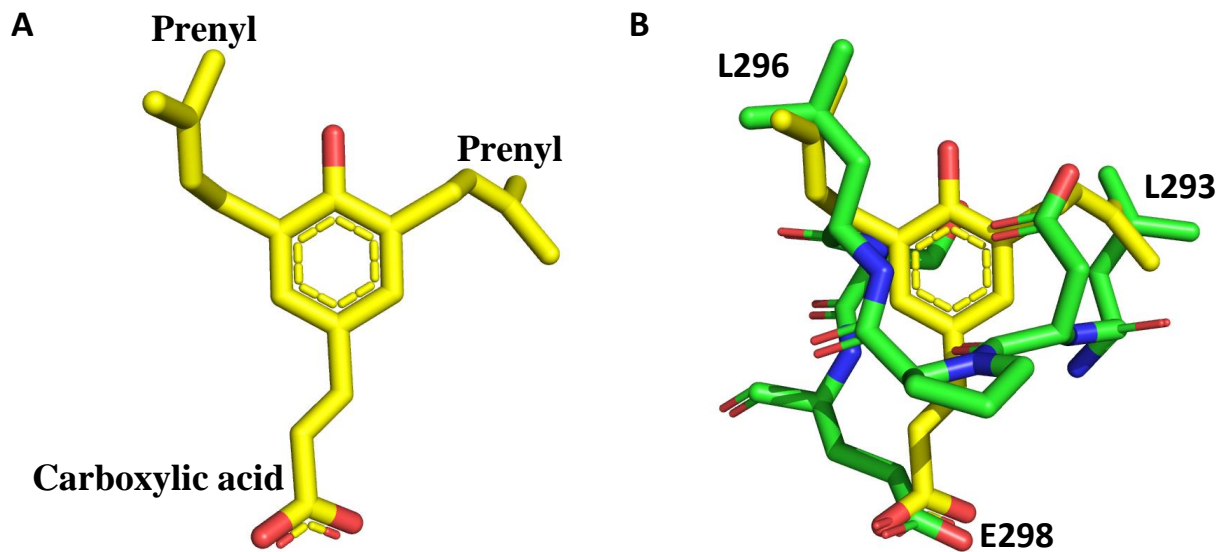


418

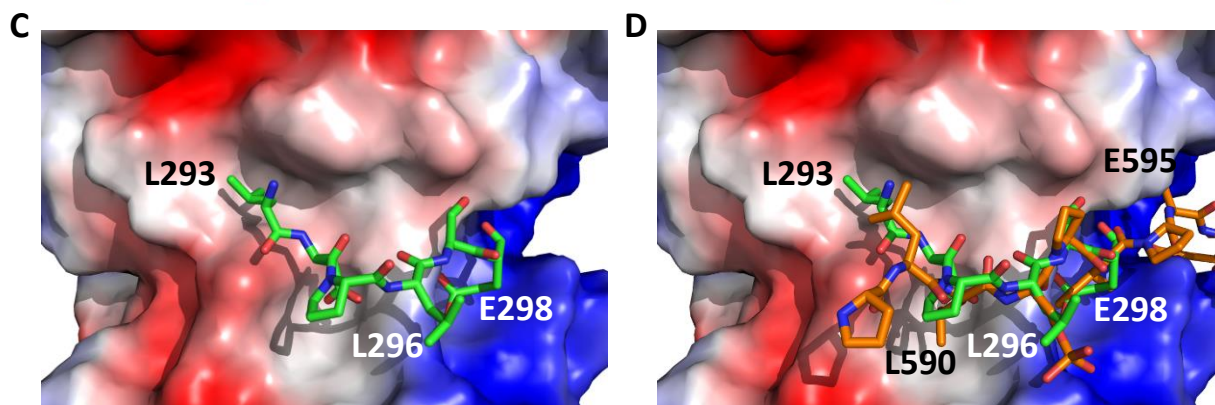
419 **Fig. 3**

420

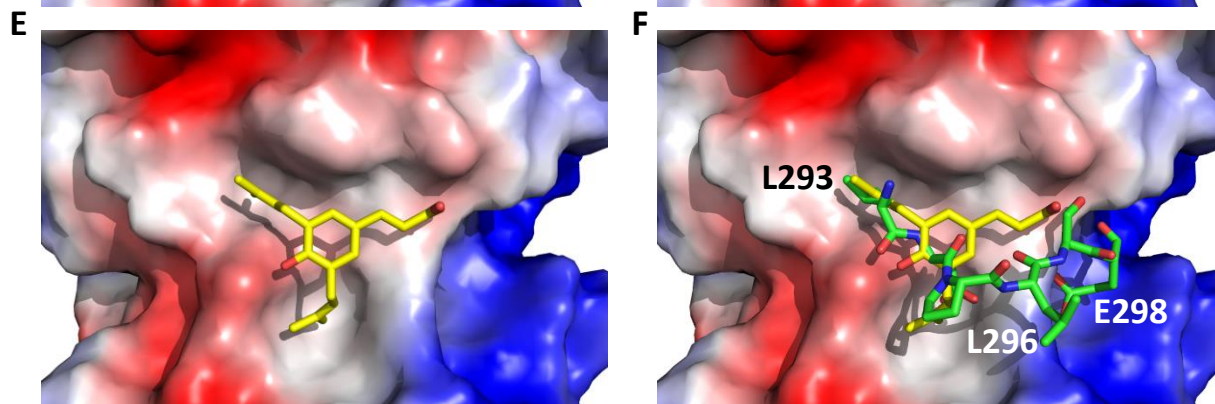
421



422



423



424

425

426 **Fig. 4**

427